

Relation between the Polyakov loop and the chiral order parameter at strong coupling

Kenji Fukushima*

Department of Physics, University of Tokyo, 7-3-1 Hongo, Bunkyo-ku, Tokyo 113-0033, Japan

We discuss the relation between the Polyakov loop and the chiral order parameter at finite temperature by using the Gocksch-Ogilvie model with fundamental or adjoint quarks. The model is based on the double expansion of strong coupling and large dimensionality on the lattice. In an analytic way with the mean field approximation employed, we show that the confined phase must be accompanied by the spontaneous breaking of the chiral symmetry for both fundamental and adjoint quarks. Then we proceed to numerical analysis to look into the coupled dynamics of the Polyakov loop and the chiral order parameter. In the case of fundamental quarks, the pseudo-critical temperature inferred from the Polyakov loop behavior turns out to coincide with the pseudo-critical temperature of the chiral phase transition. We discuss the physical implication of the coincidence of the pseudo-critical temperatures in two extreme cases; one is the deconfinement dominance and the other is the chiral dominance. As for adjoint quarks, the deconfinement transition of first order persists and the chiral phase transition occurs distinctly at higher temperature than the deconfinement transition does. The present model study gives us a plausible picture to understand the results from the lattice QCD and aQCD simulations.

PACS numbers: 11.10.Wx, 11.15.Me, 11.30.Rd, 12.38.Lg

I. INTRODUCTION

Recent developments in the heavy ion collision experiment are going to enable us to reach phase transitions that the early universe must have undergone, i.e., the phase transition from hadronic matter to a quark-gluon plasma (QGP) [1]. From the theoretical point of view what is known as the QGP phase transition can consist of two distinct phase transitions. One is the *color deconfinement transition* and the other is the *chiral symmetry restoration* or the *chiral phase transition*. The color liberation associated with deconfinement is a phenomenon distinguishable from the chiral phase transition in principle, but it is likely that the mechanism of confinement would be closely related to the chiral dynamics. According to several theoretical studies [2], in fact, confinement should be accompanied by the spontaneous chiral symmetry breaking. In other words, the critical temperature relevant to the deconfinement transition (denoted by T_d) is inevitably lower than that relevant to the chiral phase transition (denoted by T_χ), that is; $T_d \leq T_\chi$, if two phase transitions are to be distinguished.

Actually it is difficult to shed light on underlying physics in the relation between two phase transitions. It is partly because most of the effective models involving the chiral dynamics have shortcomings in describing confinement physics, and partly because the criterion to characterize the deconfinement transition cannot go together with the realization of the chiral symmetry. We can define an order parameter for the deconfinement transition only when there is no dynamical quark in a theory, or quarks are infinitely massive ($m_q \rightarrow \infty$). In contrast to it, the chiral symmetry is manifested when quarks can be regarded as massless ($m_q \sim 0$). Thus two phase transitions must lie in the opposite limits in regard to the current quark mass.

In the absence of dynamical quarks pure gluonic systems have the center symmetry and the Polyakov loop, L , provides a criterion for confinement [3, 4]. The expectation value of the Polyakov loop traced in the fundamental representation can be related to the free energy f_q with a static fundamental quark placed in a thermal medium, that is; $\langle \text{Tr}_c L \rangle = \exp[-\beta f_q]$, where Tr_c denotes the trace over the color space and β is the inverse temperature [38]. Under the center transformation the traced Polyakov loop, $\text{Tr}_c L$, is twisted by an element of the center group (i.e. the $Z(N_c)$ group for an $SU(N_c)$ gauge theory). In the confined phase where $f_q = \infty$, the center symmetry is realized to result in $\langle \text{Tr}_c L \rangle = 0$, while the spontaneous breaking of the center symmetry occurs in the deconfined phase where the expectation value of the Polyakov loop takes a finite value corresponding to $f_q < \infty$.

For the purpose of looking into the spontaneous breaking of the center symmetry, the effective action in terms of the Polyakov loop has been pursued by the strong coupling expansion as well as by the perturbative calculation. Indeed, it has been revealed that the center symmetry is spontaneously broken in a perturbative regime at high temperature, which is actually embodied in what is often called the Weiss potential [7]. As the temperature is lowered, unstable

*Electronic address: fuku@nt.phys.s.u-tokyo.ac.jp

modes can develop to make the expectation value of the Polyakov loop diminished [8]. Unfortunately, however, we cannot reach an appropriate description of the deconfinement transition in any perturbative way because the phase transition is a non-perturbative phenomenon and moreover the perturbative calculation would have no information on the Haar measure [8, 9]. The Haar measure in the context of confinement physics means a sort of the Faddeev-Popov determinant [10], or precisely speaking, the Jacobian of the variable transformation from the gauge potential to the Polyakov loop. As stressed also in Ref. [11], the nature of the group integration contained in the Haar measure can be responsible for confinement and, in fact, it is the case in the strong coupling expansion on the lattice. It has been found that the resultant effective action in the lowest order of the strong coupling expansion leads to a second order phase transition for the SU(2) gauge theory [12] and a first order phase transition for the SU($N_c \geq 3$) gauge theories [13]. These results in the strong coupling expansion are consistent with the anticipation derived from the analogy to spin systems based on the center symmetry [3]. They are in agreement with the results from the lattice simulation as well [4].

When massless quarks in the fundamental representation are present in a theory, the center symmetry is broken explicitly and the Polyakov loop would no longer serve as an order parameter to identify the deconfinement transition [14]. Then, another symmetry, i.e., the chiral symmetry plays an important role in hadronic properties. There are many effective approaches based on the chiral symmetry such as the linear-sigma model, the Nambu–Jona-Lasinio model, the chiral random matrix model and so on [15]. The spontaneous breaking of the chiral symmetry with the staggered fermion on the lattice has already been investigated by means of the double expansion of strong coupling and large dimensionality [16, 17]. The results are surprisingly acceptable not only qualitatively but quantitatively also.

For a moderate value of the quark mass, neither the deconfinement transition nor the chiral phase transition has any well-defined order parameter. In the lattice QCD simulation, it has been observed that the Polyakov loop and the chiral order parameter show crossover behaviors in the presence of dynamical quarks [18], as if the magnetization in spin systems under an external magnetic field. To be interesting, the lattice QCD results suggest that the simultaneous transitions for deconfinement and chiral restoration take place at the same pseudo-critical temperature, that is; the respective peaks of the susceptibility for the Polyakov loop and for the chiral order parameter are found at the same temperature.

In Ref. [19], Satz emphasized that such coincidence of the pseudo-critical temperatures can be understood in the following way: At low temperature where the chiral symmetry is spontaneously broken, the explicit breaking of the center symmetry is suppressed by the heavier mass of constituent quarks rather than the lighter mass of current quarks. Consequently the expectation value of the Polyakov loop stays small in the confined or chiral broken phase at low temperature. Once the constituent quark mass drops off in the chiral symmetric phase at high temperature, the explicit breaking of the center symmetry is enlarged to result in a finite value of the Polyakov loop. Although this qualitative argument is developed further in Ref. [20], any quantitative demonstration had not been given until our analysis on the Gocksch-Ogilvie model [21, 22]. It should be noticed that, according to Satz’s argument, the behavior of the Polyakov loop would be sensitive to the chiral phase transition rather than the deconfinement transition. In order to disclose the underlying relation between deconfinement and chiral restoration, some legitimate order parameters are indispensable to characterize the deconfinement transition even in the presence of dynamical quarks. However, defining an order parameter for the deconfinement transition is a quite difficult question because of the thermal excitation of dynamical quarks, particularly under the thermodynamic limit at finite temperature [23].

Alternatively, it is interesting to consider the system with dynamical quarks in the adjoint representation since adjoint quarks would preserve the center symmetry. Actually the color structure of adjoint quarks is identical to that of gluons. Thus the Polyakov loop serves as an appropriate order parameter for the deconfinement transition with respect to *fundamental* quarks in a similar way as in the pure gluonic theories. The chiral phase transition for dynamical adjoint quarks and the deconfinement transition for static fundamental quarks can be defined separately in this case. In the lattice simulation with adjoint quarks (lattice aQCD), it has been found that the critical temperature for the chiral restoration is distinctly higher than that for the deconfinement transition [24]. In this paper we apply the Gocksch-Ogilvie model to investigate the system with adjoint quarks as well.

This paper is organized as follows: We explain what the Gocksch-Ogilvie model is with emphasis on its physical meaning in Sec. II. We give computational details in App. A additionally. In Sec. III we elaborate the mean field approximation employed in the present analysis. Then in an analytic way we investigate the effects on the chiral dynamics arising from the Polyakov loop behaviors. Sec. IV is devoted to presenting the numerical results and discussing their physical implications. Finally, we conclude our model study in Sec. V.

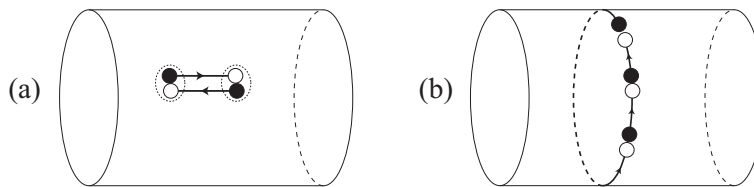


FIG. 1: Intuitive pictures for the effective action of the Goksch-Ogilvie model. The torus consists of the thermal S^1 and the spatial R^3 . The arrowed line represents the link variable. The filled and blank circles are the quark and anti-quark excitations. (a) In the spatial directions a quark and an anti-quark propagate as a meson as a result of the group integration with respect to the spatial link variables. (b) Thermal excitations of dynamical quarks are allowed by the non-vanishing Polyakov loop at finite temperature.

II. GOCKSCH-OGILVIE MODEL

The Goksch-Ogilvie model is given by the effective action [21, 22]; (see App. A for detail derivations)

$$S_{\text{eff}}^{(r)}[L, \lambda] = -J \sum_{\text{n.n.}} \text{Tr}_c L(\vec{n}) \text{Tr}_c L^\dagger(\vec{m}) + \frac{\dim(r)}{2} \sum_{m,n} \lambda(n) V(n, m) \lambda(m) - \frac{N_f}{4} \sum_{\vec{n}} \text{Tr}_c \ln \left[\cosh(N_\tau E) + \frac{1}{2} (L^{(r)} + L^{(r)\dagger}) \right], \quad (1)$$

where $L(\vec{n})$ is the Polyakov loop in the fundamental representation defined on the lattice by

$$L(\vec{n}) = \prod_{n_d=a}^{N_\tau a} U_d(\vec{n}, n_d) \quad (2)$$

in the d dimensional space-time. $L^{(r)}$ denotes the Polyakov loop in the r representation ($r = \text{fund.}$ for the fundamental representation and $r = \text{adj.}$ for the adjoint one). The Polyakov loop in the adjoint representation can be expressed in terms of the fundamental ones as

$$L_{ab}^{(\text{adj.})} = 2 \text{tr} \left[t_a L t_b L^\dagger \right], \quad (3)$$

where the matrices t_a form a fundamental representation of the $SU(N_c)$ group and the indices a, b run from 1 to $N_c^2 - 1$. The normalization is determined to satisfy $\text{tr}[t_a t_b] = \delta_{ab}/2$.

In the effective action (1), $\lambda(n)$ is the meson field, Tr_c the trace with respect to the color indices, and N_f the number of flavors which is taken as $N_f = 2$ throughout this paper. $\dim(r)$ is the number of dimension in the r representation of the $SU(N_c)$ group, that is; $\dim(\text{fund.}) = N_c$ and $\dim(\text{adj.}) = N_c^2 - 1$. The temperature T , the meson hopping propagator $V(n, m)$, the strength of the nearest neighbor interaction J , and the quasi-quark energy (constituent quark mass) E are defined respectively as

$$T = \frac{1}{N_\tau a}, \quad V(n, m) = \frac{1}{2(d-1)} \sum_{\hat{j}} (\delta_{n, m+\hat{j}} + \delta_{n, m-\hat{j}}),$$

$$J = e^{-\sigma a/T}, \quad E = \sinh^{-1} \left(\sqrt{\frac{d-1}{2}} \lambda + m_q \right) \quad (4)$$

with \hat{j} running from 1 to $d-1$ only in the spatial directions. σ stands for the string tension fixed at the empirical value at zero temperature, i.e., $\sigma = (425 \text{ MeV})^2$. The lattice spacing a and the current quark mass m_q are treated as the model parameters.

Physical meaning for each term in the effective action (1) is straightforward to understand. The first term is the gluonic contribution in terms of the Polyakov loop. An order-disorder phase transition described by this gluonic action signifies the transition from the center symmetric confined phase to the symmetry broken deconfined phase. The next term involving $\lambda(n)$ is the meson interaction term in the spatial direction resulting from the group integration with respect to the spatial link variables as shown in Fig. 1 (a). The last logarithmic term corresponds to the thermal excitation of dynamical quarks as depicted intuitively in Fig. 1 (b). This interpretation will become tangible if once

the Polyakov loop $L^{(r)}$ is set to be unity by hand. The logarithmic term then takes a familiar form of the free energy for fermionic ideal gases.

In the case of fundamental quarks the center symmetry is explicitly broken by the thermal quark excitation with fractional baryon number. Actually the expansion of the logarithmic quark contribution in the power of the Polyakov loop is essentially equivalent to the hopping parameter expansion [25] and then the power of the Polyakov loop counts the winding number of quark paths along the thermal torus, namely, the quark number in the system. The leading contribution in such an expansion in terms of the Polyakov loop is $\sim \text{Tr}_c L / \cosh(N_\tau E)$, which can be regarded as the symmetry breaking term under an external magnetic-like field in analogy to spin systems. The magnitude of the symmetry breaking external field is specified by $1/\cosh(N_\tau E)$ hence it becomes smaller as the constituent quark mass gets larger. Thus Satz's argument on the relation between the Polyakov loop behavior and the chiral dynamics is already embodied qualitatively in the Gocksch-Ogilvie model in a natural way. Of course, the model will give us deeper insight into the interplay between the deconfinement transition and the chiral phase transition beyond qualitative arguments, as we will see in the subsequent sections.

Now we shall remark about the applicable range in which the Gocksch-Ogilvie model can make sense. The limit of the temperature going to zero would render the model illegitimate because separate treatments for the spatial directions and for the thermal direction as illustrated in Fig. 1 can be allowed safely only at high temperature. In order to take the limit of zero temperature properly in the Gocksch-Ogilvie model, the group integration with respect to the Polyakov loop, as performed in Ref. [17], is indispensable, which needs somewhat complicated algebraic procedures. The interested temperature here is, as we will see later, around 200 MeV which corresponds to $N_\tau \sim 2$ in the present analysis. Thus we believe that it is well-founded to deal with the thermal direction separately in the construction of the model. The opposite limit of the temperature getting extremely high would make the quantitative argument meaningless simply because the strong coupling expansion does not work in a perturbative regime at such high temperature. The Stefan-Boltzmann law, for example, cannot be derived within the framework of the strong coupling expansion on the lattice. In any case, as far as the region around the critical temperature is concerned, we can presume that the Gocksch-Ogilvie model should be applicable.

III. ANALYTIC CALCULATIONS

A. Mean-Field Approximation

The dynamics of the Polyakov loop can be understood in analogy to spin systems with the center symmetry. As usually performed in the calculation in the spin system, we will adopt the mean field (Weiss) approximation for the Polyakov loop. In this approximation, we take account of the fluctuation of the individual Polyakov loop surrounded by a constant mean field around it. The mean field action is taken here as

$$S_{\text{mf}}[L] = -\frac{x}{2} \sum_{\vec{n}} \{ \text{Tr}_c L(\vec{n}) + \text{Tr}_c L^\dagger(\vec{n}) \}, \quad (5)$$

where x is the mean field for the Polyakov loop and treated as a variational parameter to be determined afterward from the extremal condition on the free energy. As for the chiral order parameter, λ is simply regarded as a constant mean field denoted by $\bar{\lambda}$. The mean field free energy is then given by [26]

$$\begin{aligned} \beta f_{\text{mf}}^{(r)}(x, \bar{\lambda}) &= -N^{-(d-1)} \left(\langle -S_{\text{eff}}^{(r)}[L, \bar{\lambda}] + S_{\text{mf}}[L] \rangle_{\text{mf}} + \ln \int \mathcal{D}L e^{-S_{\text{mf}}[L]} \right) \\ &= \beta f_{\text{gluon}}(x) + \beta f_{\text{quark}}^{(r)}(x, \bar{\lambda}). \end{aligned} \quad (6)$$

Here $\langle \dots \rangle_{\text{mf}}$ means the expectation value with the weight specified by the mean field action. $N^{(d-1)}$ is the spatial volume. Roughly speaking, the first term $\langle S_{\text{eff}}^{(r)} \rangle_{\text{mf}}$ corresponds to the internal energy tending to make the system ordered and remaining terms are the entropy tending to make the system disordered.

The gluonic part of the free energy can be written as

$$\beta f_{\text{gluon}}(x) = -2(d-1)J \left(\frac{d}{dx} \ln I(x) \right)^2 + x^2 \frac{d}{dx} \left(\frac{1}{x} \ln I(x) \right), \quad (7)$$

where $I(x)$ is defined by [27]

$$I(x) = \int dL \exp \left[\frac{x}{2} \text{Tr}_c (L + L^\dagger) \right] = \sum_m \det I_{m-i+j}(x) \quad (8)$$

with $I_n(x)$ representing the modified Bessel function of the first kind. The quark part of the free energy in the r representation is written for $N_f = 2$ as

$$\beta f_{\text{quark}}^{(r)}(x, \bar{\lambda}) = \frac{\dim(r)N_\tau}{2} \bar{\lambda}^2 - \frac{\dim(r)}{2} \ln[\cosh(N_\tau E)] - \frac{1}{2} \frac{\tilde{I}^{(r)}(x; \cosh(N_\tau E))}{I(x)}. \quad (9)$$

$\tilde{I}^{(r)}(x; \alpha)$ is given in the fundamental and in the adjoint representation respectively by

$$\begin{aligned} \tilde{I}^{(\text{fund.})}(x; \alpha) &= \frac{1}{N_c!} \sum_{a=1}^{N_c} \sum_{m=-\infty}^{\infty} \epsilon_{i_1 \dots i_{N_c}} \epsilon_{j_1 \dots j_{N_c}} I_{m-i_1+j_1}(x) \cdots \tilde{I}_{m-i_a+j_a}(x; \alpha) \cdots I_{m-i_{N_c}+j_{N_c}}(x), \\ \tilde{I}_n(x; \alpha) &= \int_0^{2\pi} \frac{d\phi}{2\pi} \ln \left[1 + \frac{\cos \phi}{\alpha} \right] \cos(n\phi) e^{x \cos \phi}, \end{aligned} \quad (10)$$

and

$$\begin{aligned} \tilde{I}^{(\text{adj.})}(x; \alpha) &= \frac{1}{N_c!} \sum_{a \neq b=1}^{N_c} \sum_{m=-\infty}^{\infty} \epsilon_{i_1 \dots i_{N_c}} \epsilon_{j_1 \dots j_{N_c}} I_{m-i_1+j_1}(x) \cdots \tilde{I}_{m-i_a+j_a}^{m-i_b+j_b}(x; \alpha) \cdots I_{m-i_{N_c}+j_{N_c}}(x) \\ &\quad + (N_c - 1) \ln \left[1 + \frac{1}{\alpha} \right] I(x), \\ \tilde{I}_n^m(x; \alpha) &= \int_0^{2\pi} \frac{d\phi_a d\phi_b}{(2\pi)^2} \ln \left[1 + \frac{\cos(\phi_a - \phi_b)}{\alpha} \right] \cos(m\phi_a + n\phi_b) e^{x(\cos \phi_a + \cos \phi_b)} \\ &= \int_0^{2\pi} \frac{d\phi}{2\pi} \ln \left[1 + \frac{\cos \phi}{\alpha} \right] \cos\left(\frac{m-n}{2}\phi\right) I_{m+n}\left(2x \cos \frac{\phi}{2}\right). \end{aligned} \quad (11)$$

In Eqs. (10) and (11) the integration in terms of ϕ originates from the thermal excitation of fundamental quarks. Since the excitation of an adjoint quark consists of a fundamental quark and anti-quark pair (see Eq. (3)), two integration variables ϕ_a and ϕ_b appear in Eq. (11).

Now that we have the actual expressions for the mean field free energy given by Eqs. (7) and (9), all we have to do is find the minimum of the free energy with respect to the variational parameters x and $\bar{\lambda}$. Before addressing the numerical analyses, we shall look into the analytic expressions of the free energy further in the next subsection.

B. Chiral Symmetry Breaking in the Confined Phase

It would be worth considering the particular cases where we can manipulate the mean field free energy in analytic ways. In this and the next subsections we take the chiral limit, namely, $m_q = 0$ and discuss what becomes of the chiral symmetry in some particular cases.

An interesting limit is that the mean field for the Polyakov loop is forced to be zero by hand, i.e., $x = 0$. This limit readily corresponds to the confined phase for adjoint quarks because the Polyakov loop serves as the order parameter for the deconfinement transition in the system with adjoint quarks preserving the center symmetry. To be interesting, even for fundamental quarks, the limit of $x = 0$ should indicate the confined phase. The reason is as follows; the group integration with respect to the Polyakov loop would pick out only color singlet combinations in the integrand. In the limit of $x = 0$, i.e., without any external source from the mean field, the expansion of the logarithmic contribution in terms of the Polyakov loop gives rise to only center symmetric combinations. Actually, the condition of $x = 0$ leads to the description in the canonical ensemble with the quark triality fixed at zero (see Ref. [23] and references therein). The criterion for the deconfinement transition, therefore, regains its meaning based on the center symmetry and it follows that the vanishing Polyakov loop signifies the confined phase even for fundamental quarks.

For the quark part of the free energy, taking $x = 0$ makes the expressions of Eqs. (10) and (11) simplified as

$$\tilde{I}^{(\text{fund.})}(0; \alpha) = N_c \tilde{I}_0(0; \alpha) - 2(-1)^{N_c} \tilde{I}_{N_c}(0; \alpha) \quad (12)$$

$$\tilde{I}^{(\text{adj.})}(0; \alpha) = N_c(N_c - 1) \tilde{I}_0(0; \alpha) - \sum_{a \neq b=1}^{N_c} \tilde{I}_{a-b}(0; \alpha). \quad (13)$$

Then we can make use of the following integrations [39],

$$\begin{aligned}\tilde{I}_0(0; \alpha) &= \int_0^{2\pi} \frac{d\phi}{2\pi} \ln \left[1 + \frac{\cos \phi}{\alpha} \right] = \ln \left[\frac{\alpha + \sqrt{\alpha^2 - 1}}{2\alpha} \right] \\ \tilde{I}_n(0; \alpha) &= \int_0^{2\pi} \frac{d\phi}{2\pi} \ln \left[1 + \frac{\cos \phi}{\alpha} \right] \cos(n\phi) = -\frac{1}{n} (\sqrt{\alpha^2 - 1} - \alpha)^n \quad (n \neq 0)\end{aligned}\quad (14)$$

to come by the expanded form of the free energy in terms of $\bar{\lambda}$ as [40]

$$\beta f_{\text{mf}}^{(\text{fund.})}(0, \bar{\lambda}) \simeq (\text{const.}) - \sqrt{\frac{d-1}{2}} \left(\frac{N_c}{2} - 1 \right) N_\tau |\bar{\lambda}| + \text{O}(\bar{\lambda}^2), \quad (15)$$

$$\beta f_{\text{mf}}^{(\text{adj.})}(0, \bar{\lambda}) \simeq (\text{const.}) - \sqrt{\frac{d-1}{2}} \left[\frac{N_c^2}{2} \right] N_\tau |\bar{\lambda}| + \text{O}(\bar{\lambda}^2), \quad (16)$$

where $[\dots]$ in Eq. (16) denotes the greatest integer function which gives the greatest integer less than or equal to the number. To derive the above expressions, we have substituted $\alpha = \cosh(N_\tau E) \simeq 1 + (d-1)N_\tau^2 \bar{\lambda}^2/4$.

Here we should emphasize the appearance of a linear term of $|\lambda|$ which stems from the expansion of $\sqrt{\alpha^2 - 1}$. Such a linear term always causes instability around the chiral symmetric vacuum ($\bar{\lambda} = 0$). In other words, we have shown from Eqs. (15) and (16) that the Gocksch-Ogilvie model with the mean field approximation has the property that *the chiral symmetry is inevitably broken spontaneously in the confined phase* for both fundamental and adjoint quarks. This property is in accordance with the general theoretical requirement.

C. Chiral Restoration Temperature

We can now consider the opposite situation where the Polyakov loop is almost trivial in the deconfined phase and the chiral restoration occurs continuously. Then, as discussed in Refs. [21, 22], we can acquire the chiral restoration temperature by the quadratic term of the free energy expanded in terms of the chiral order parameter $\bar{\lambda}$. Supposing that the mean field for the Polyakov loop takes a substantially finite value, let us assume that the Polyakov loop can be approximated simply by $L_{ij} \simeq v \cdot \delta_{ij}$ and $L_{ab}^{(\text{adj.})} \simeq v^2 \cdot \delta_{ab}$, though this approximation breaks the unitarity of the matrices L and $L^{(\text{adj.})}$. The free energies for fundamental and adjoint quarks are expanded up to the quadratic order as

$$\beta f_{\text{quark}}^{(\text{fund.})}(L = v, \bar{\lambda}) \simeq (\text{const.}) + \frac{N_c N_\tau}{2} \left[1 - \frac{(d-1)N_\tau}{4(v+1)} \right] \bar{\lambda}^2 + \text{O}(\bar{\lambda}^4), \quad (17)$$

$$\beta f_{\text{quark}}^{(\text{adj.})}(L = v, \bar{\lambda}) \simeq (\text{const.}) + \frac{(N_c^2 - 1)N_\tau}{2} \left[1 - \frac{(d-1)N_\tau}{4(v^2+1)} \right] \bar{\lambda}^2 + \text{O}(\bar{\lambda}^4). \quad (18)$$

From these expansions, we can immediately have the chiral restoration temperatures;

$$T_\chi^{(\text{fund.})} = \frac{d-1}{4(v+1)} a^{-1}, \quad T_\chi^{(\text{adj.})} = \frac{d-1}{4(v^2+1)} a^{-1}. \quad (19)$$

In contrast to the lattice observation [24], the chiral restoration temperature for adjoint quarks is not changed radically from that for fundamental quarks. From the analytic expressions for the critical temperature we can see the tendency that the chiral restoration should be hindered as the system approaches the confined phase where $v \sim \langle \text{Tr}_c L \rangle$ gets smaller, though the above expressions are only valid for $v \sim 1$.

D. Modification to the Deconfinement Temperature

Although the angle integrations appearing in Eqs. (10) and (11) seem too complicated to accomplish analytically, the expansion in terms of $1/\alpha$, which will be acceptable when the quark mass is large, enables us to write down $\tilde{I}_n(x; \alpha)$ and $\tilde{I}_n^m(x; \alpha)$ immediately (see also App. D). Such an expansion in the leading order of $1/\alpha$ and a further

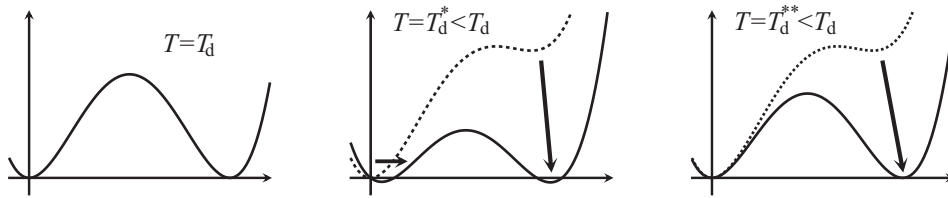


FIG. 2: Schematic figures to show the modification to the free energy. The left figure is for the first order transition at $T = T_d$ in the pure gluonic case. The transition temperature is lowered from T_d to T_d^* and the minimum around the origin is shifted by the linear term for fundamental quarks (middle figure). The transition temperature is also lowered to T_d^{**} by the quadratic term for adjoint quarks (right figure).

expansion in terms of x as well yield the following expressions of the free energy for $N_c = 3$;

$$\beta f_{\text{gluon}}(x) \simeq -2(d-1)J \left(\frac{x}{2} + \frac{x^2}{8} - \frac{5x^4}{384} - \frac{x^5}{256} \right)^2 + \frac{x^2}{4} + \frac{x^3}{12} - \frac{x^5}{96} - \frac{5x^6}{1536}, \quad (20)$$

$$\beta f_{\text{quark}}^{(\text{fund.})}(x, \bar{\lambda}) \simeq \frac{3}{2}N_\tau \bar{\lambda}^2 - \frac{3}{2} \ln \cosh(N_\tau E) - \frac{1}{2 \cosh(N_\tau E)} \left(\frac{x}{2} + \frac{x^2}{8} - \frac{5x^4}{384} - \frac{x^5}{256} \right), \quad (21)$$

$$\beta f_{\text{quark}}^{(\text{adj.})}(x, \bar{\lambda}) \simeq 4N_\tau \bar{\lambda}^2 - 4 \ln \cosh(N_\tau E) - \frac{1}{2 \cosh(N_\tau E)} \left(\frac{x^2}{4} + \frac{x^3}{12} - \frac{x^5}{96} \right). \quad (22)$$

The gluonic part of the free energy always has a minimum around $x = 0$ because the expansion starts from the order of x^2 . Thus it can describe the first order deconfinement transition from $x = 0$ to some finite x at the deconfinement temperature T_d as shown schematically in the left figure of Fig. 2. The absence of the linear term of x reflects the center symmetric property.

The expansion (21) for fundamental quarks clearly shows that the quark contribution breaks the center symmetry through the linear term of x . In the presence of such a linear term, the minimum around $x = 0$ in the gluonic free energy is shifted to a finite value of x . As far as only the linear term, which is negative now, is concerned, the free energy will be more decreased at larger x . As a result, the first order deconfinement transition temperature is lowered from T_d to $T_d^* < T_d$ by the effect of the explicit breaking of the center symmetry, if the first order transition persists. The intuitive picture is depicted in the middle figure of Fig. 2. As a matter of fact, the first order transition occurs even in the presence of dynamical quarks with $m_q \gtrsim 300$ MeV for Parameter I and $m_q \gtrsim 700$ MeV for Parameter II (the meaning of the model parameters is given in the next section).

In Eq. (22), on the other hand, the leading term from the logarithmic contribution is quadratic in x and the minimum around $x = 0$ is not altered then. This is because of the center symmetry remaining for adjoint quarks. When we focus attention on the leading term, as in the above case for fundamental quarks, the negative contribution of order x^2 in the quark free energy will reduce the free energy more for larger x . Therefore, as shown in the right figure of Fig. 2, the first order deconfinement transition temperature is also lowered to $T_d^{**} < T_d$ in the presence of adjoint quarks.

The strength of how much the deconfinement temperature is lowered, i.e., $T_d - T_d^*$ or $T_d - T_d^{**}$, is specified by $\sim 1/\cosh(N_\tau E)$. As long as the current quark mass, m_q , is smaller than the scalar condensate $\bar{\lambda}$, or as long as the constituent quark mass Ea^{-1} is smaller than the temperature $T = 1/N_\tau a$, the modification to the deconfinement temperature will be almost insensitive to m_q . This anticipation, in fact, has been observed in the lattice aQCD simulations [24] and will be confirmed in our numerical results in the next section.

IV. NUMERICAL RESULTS AND DISCUSSIONS

The parameters inherent in the Gocksch-Ogilvie model are the lattice spacing (cut-off) a and the current quark mass m_q . In our previous work [22], a and m_q are chosen to fit the masses of pions and ρ mesons. If m_q is much smaller than a^{-1} then a is essentially determined by the mass difference between pions and ρ mesons and m_q is fixed by the condition to reproduce the pion mass. The numerical values of the model parameters in this case are listed as Parameter I in Table I. The deconfinement transition in a pure gluonic system occurs at $2(d-1)J_c = 0.806$, that is; $T_d = 208$ MeV with these values of the model parameters. This value of T_d seems to be rather low as compared with the empirical value ($T_d = 270$ MeV) found in the lattice simulations. Since the transition temperatures are crucial rather than the hadron spectrum here, we will try another parameter set, Parameter II, in this paper; instead of using the ρ meson mass, we can fix the lattice spacing a so as to reproduce the empirical value of the deconfinement

	a^{-1}	m_q	m_π	m_ρ	Ψ	T_d	T_c
Parameter I	432 MeV	5.7 MeV	*140 MeV	*770 MeV	$-(342 \text{ MeV})^3$	208 MeV	$\sim 187 \text{ MeV}$
Parameter II	333 MeV	7.4 MeV	*140 MeV	597 MeV	$-(263 \text{ MeV})^3$	*270 MeV	$\sim 230 \text{ MeV}$

TABLE I: Model parameters employed in the numerical calculations and the resultant outputs. *-quantities are used as inputs in order to fix a and m_q . Ψ is the chiral condensate.

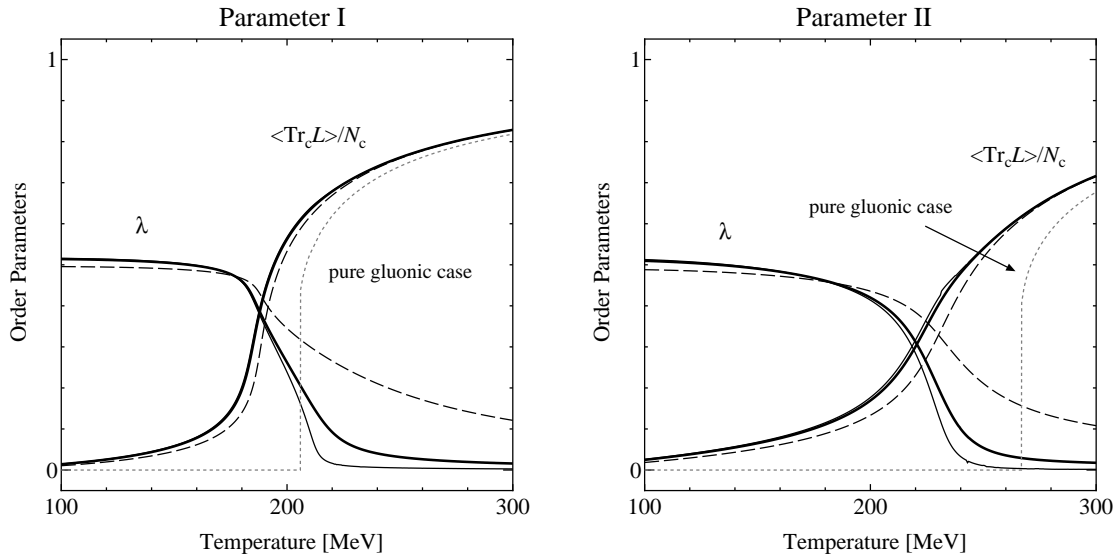


FIG. 3: Behaviors of the order parameters as functions of the temperature for $N_c = 3$. The thick solid curve is for $m_q = 5.7 \text{ MeV}$ in the left figure (Parameter I) and for $m_q = 7.4 \text{ MeV}$ in the right figure (Parameter II). The thin solid curve is for $m_q = 1 \text{ MeV}$ and the dashed curve for $m_q = 50 \text{ MeV}$.

transition temperature by substituting J_c and the empirical T_d for Eq. (4). We summarize our choice of the model parameters and the resultant outputs in Table I. As we will discuss later, these two parameter sets (Parameter I and Parameter II) happen to correspond to two typical cases for the realization of the simultaneous phase transitions.

It should be noted that we have determined the model parameters by using the expressions of the hadron masses at zero temperature according to Ref. [16], instead of those achieved in the zero temperature limit of the Gocksch-Ogilvie model. We briefly review the necessary expressions at zero temperature with modifications for N_f flavors in App. C. In order to take the zero temperature limit of the Gocksch-Ogilvie model we have to integrate out the Polyakov loop variable properly. It is, however, a somewhat subtle procedure and thus we choose to use the would-be solutions at zero temperature from the beginning. Actually the numerical value of the model parameters fixed in this way turns out to be almost the same as that fixed by the approximate zero temperature limit (without the Polyakov loop integration) of the Gocksch-Ogilvie model as actually adopted in Ref. [21].

The numerical results for $N_c = 3$ are presented in Fig. 3 together with the results for several different choices of the current quark mass. In the presence of quark contributions, the expectation value of the Polyakov loop is not equal to x itself, though in the pure gluonic case the extremal condition on the free energy ensures that the mean field for the Polyakov loop is simply provided by x . From Eqs. (5) and (8) we can have the following relation;

$$\frac{1}{2N_c} \langle \text{Tr}_c L + \text{Tr}_c L^\dagger \rangle = \frac{1}{N_c} \frac{dI(x)}{dx}, \quad (23)$$

from which we have calculated the expectation value of the Polyakov loop. As for the chiral order parameter, we simply use the scalar condensate $\bar{\lambda}$, for we can show that it is proportional to the conventional order parameter, i.e., the chiral condensate $\Psi = \langle \bar{\chi}\chi \rangle$. Further details are given in App. B.

In both cases of Parameter I and Parameter II, we can see the order parameters for deconfinement and chiral restoration indicating crossover behaviors almost simultaneously. Although the numerical results in Fig. 3 might seem just supportive for Satz's argument, the relation between the Polyakov loop and the chiral order parameter has richer contents in itself, which can be deduced from Fig. 4.

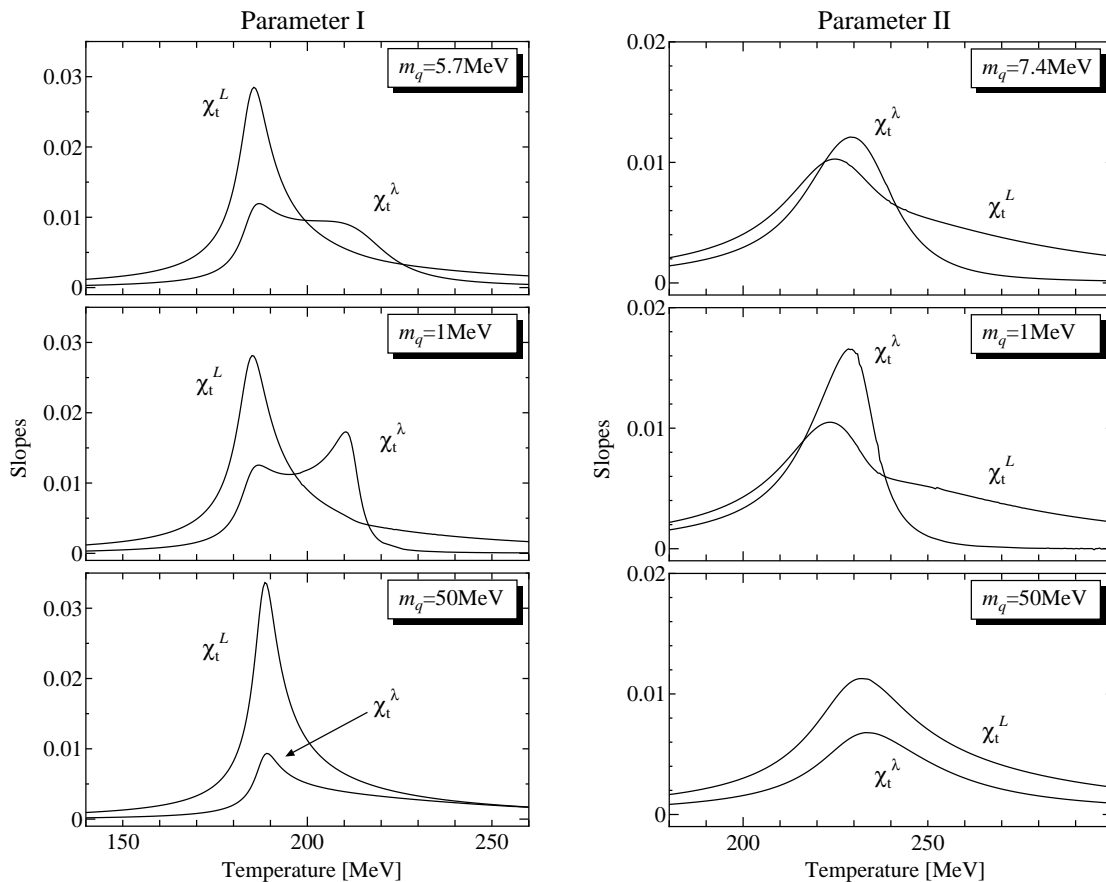


FIG. 4: Slopes (temperature derivatives) of the order parameters.

In Fig. 4 we plot the temperature derivative of the order parameters defined by

$$\chi_t^L = \frac{1}{N_c} \frac{\partial \langle \text{Tr}_c L \rangle}{\partial T}, \quad \chi_t^\lambda = -\frac{\partial \bar{\lambda}}{\partial T}, \quad (24)$$

which are nothing but the slope of the curves drawn in Fig. 3.

In both cases of the parameter sets, the pseudo-critical temperature, T_c , inferred from the peak of χ_t^L is almost identical to that from the peak of χ_t^λ . Surely the coincidence of the pseudo-critical temperatures found in the lattice QCD simulation can be reproduced in the slope of the order parameters within the present model study. It is interesting to see that the physical implication for the case of Parameter I is different from that for the case of Parameter II.

For $m_q = 1$ MeV with Parameter I, two peaks emerge apparently in the behavior of χ_t^λ . In this case one peak around $T_c \simeq 187$ MeV corresponds to the remnant of the first order deconfinement transition rather than the chiral phase transition as conjectured formerly in Ref. [22]. The other around $T \simeq 210$ MeV has the origin from the second order chiral phase transition, which can be also confirmed by the thin curve behavior in Fig. 3. Therefore the coincidence of the pseudo-critical temperatures signifies not the chiral phase transition but the induced instability of the chiral order triggered by the deconfinement transition.

For $m_q = 1$ MeV with Parameter II, on the other hand, there appears only one peak around $T_c \simeq 230$ MeV. The peak height of χ_t^λ around T_c becomes larger as the current quark mass is lowered, which is peculiar to the genuine phase transition. Therefore, this peak is considered as resulting from the second order chiral phase transition and the transition temperature, in fact, agrees with that read from the thin curve behavior in Fig. 3. Thus the coincidence of the pseudo-critical temperatures in this case can be understood according to Satz's argument.

Which transition governs the simultaneous jump around the pseudo-critical temperature relies on the magnitude relation between the chiral restoration temperature T_χ and the lowered deconfinement temperature T_d^* . In the case of Parameter I, $T_d^* < T_\chi$ is realized to lead to, so to speak, the *deconfinement dominance* around T_c . In reality, because two peaks are not observed in the lattice QCD simulation, a more relevant situation is to be described by

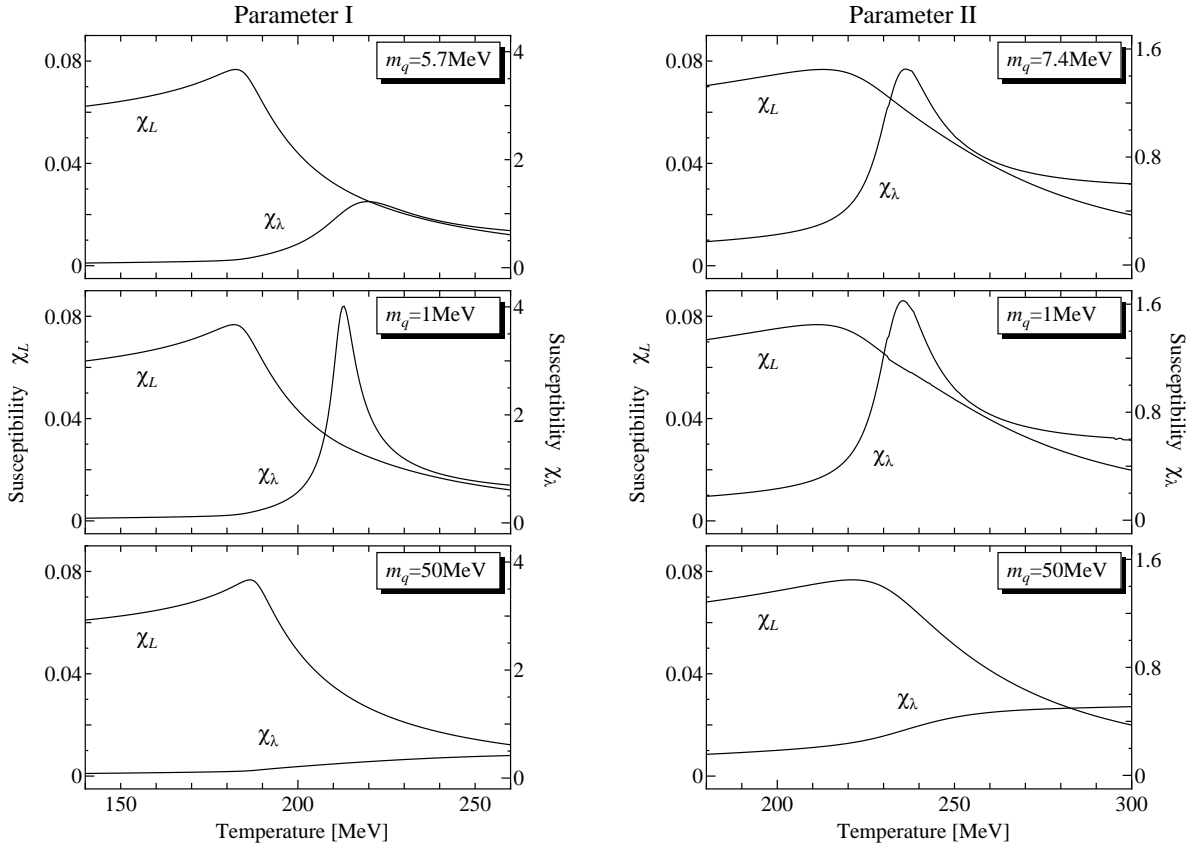


FIG. 5: Susceptibilities with respect to the order parameters.

Parameter II where $T_d^* > T_\chi$ or $T_d^* \simeq T_\chi$ would hold. The former $T_d^* > T_\chi$ means the *chiral dominance* around T_c and then the critical phenomena are to be characterized by the critical exponents associated with the chiral phase transition. However, because of the general property that the chiral phase transition must take place at higher temperature than the deconfinement transition does, as we have explained in the previous section, the latter $T_d^* \simeq T_\chi$ is likely to be realized. If it is the case, the chiral phase transition might be so affected by the remnant of the first order deconfinement transition that the critical phenomena peculiar to the second order transition would be obscured. This can be one possible account for the unsatisfactory agreement between the anticipation based on the universality argument and the critical exponents measured in the lattice QCD simulations [18].

Fig. 5 is the figure for the susceptibility with respect to the order parameters. The susceptibilities are here to be calculated by

$$\chi_L = \frac{1}{N_c^2} \left(\langle (\text{Tr}_c L)^2 \rangle - \langle \text{Tr}_c L \rangle^2 \right) = \frac{1}{N_c^2} \frac{d^2}{dx^2} \ln I(x), \quad (25)$$

$$\chi_\lambda = \langle \lambda^2 \rangle - \langle \lambda \rangle^2 = \left(\frac{\partial^2 \beta f_{\text{mf}}^{(\text{fund.})}}{\partial \lambda^2} \right)^{-1}. \quad (26)$$

The definition of χ_λ seems to be different from the conventional chiral susceptibility $\chi_\psi = \langle (\bar{\chi}\chi)^2 \rangle - \langle \bar{\chi}\chi \rangle^2$, but χ_λ is almost proportional to χ_ψ near the critical temperature as explained in App. B.

The genuine susceptibilities appear to be substantially different from the slopes and do not indicate any clear coincidence of the location of peaks. This is partly because of the very difference between the slope and the susceptibility and partly because of the approximation.

The slope χ_t^λ and the susceptibility χ_λ are certainly sensitive to the second order chiral phase transition, and yet they can have different behaviors. In the chiral limit for a clear example, the slope vanishes above the critical temperature T_χ , while the susceptibility becomes finite or even larger than the magnitude below T_χ . Actually simple mean field arguments typically give twice larger amplitude for the susceptibility above T_χ than that below T_χ .

The slope and the susceptibility relevant to the Polyakov loop, on the other hand, do not have to enhance due to the first order deconfinement transition. Therefore, for Parameter I, we have no reason to expect any coincidence

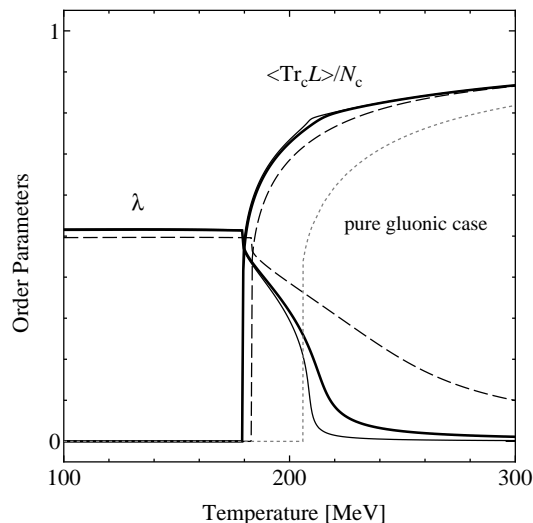


FIG. 6: Behaviors of the order parameters for adjoint quarks with Parameter I. The thick solid curve is for $m_q = 5.7$ MeV and the thin solid and the dashed curves for $m_q = 1$ MeV and for $m_q = 50$ MeV respectively.

from the beginning because of the deconfinement dominance where the Polyakov loop behavior has little information on the second order transition. The Polyakov loop behavior is still smooth even for Parameter II. We consider that it is because the simple ansatz of the mean field action (5) would miss the significant part of the coupling to the symmetry breaking contribution through which the coincidence is brought about. This ansatz can incorporate, at most, a linear term of an external magnetic-like field and thus the non-linearity leading to the fact that the chiral phase transition temperature must be higher than the deconfinement transition temperature would be lost as a result of the approximation. Hence we cannot see the coincidence of the peak location even for Parameter II.

Now we would comment upon one interesting possibility: The results from the lattice QCD simulation suggest that the situation of Parameter II is more realistic, and nevertheless, it would be appealing to consider some modification or artificial tuning in the lattice simulation, by which the case of Parameter I is realized. Then we can make use of the lattice simulation directly to investigate the nature of the deconfinement transition around T_c and the nature of the chiral phase transition around $T_\chi > T_c$ separately.

Finally we show the numerical results for adjoint quarks with Parameter I in Fig. 6. The calculation has been done with the function $\tilde{I}_n^m(x; \alpha)$ expanded in terms of $1/\alpha$ up to third order, for the numerical integration is not impossible but somewhat tough. We give the explicit expressions and verify the reliability of such an expansion in App. D. As expected, the deconfinement transition of first order persists clearly and the chiral phase transition occurs distinctly at higher temperature than the deconfinement transition does.

The global features consist well with the lattice aQCD results. The deconfinement temperature is lowered from $T_d = 208$ MeV to $T_d^{**} \simeq 180$ MeV. For various choices of m_q , the lowered deconfinement temperature T_d^{**} is almost the identical, as we have already discussed in the previous section.

The behavior of the chiral order parameter, as pointed out in Ref. [24], changes radically at $T = T_d$; the current quark mass dependence is not manifested until the temperature exceeds the deconfinement temperature. This feature can be understood qualitatively from Eq. (19). While the Polyakov loop is zero, the chiral order parameter behaves as a function of the temperature as if the chiral phase transition would take place at much higher temperature. After the deconfinement transition, the chiral restoration comes to affect the chiral order parameter behavior and, as a result, the quark mass dependence becomes apparent then.

V. CONCLUSIONS

We investigated the relation between the deconfinement transition and the chiral phase transition at finite temperature in the Gocksch-Ogilvie model with fundamental or adjoint quarks incorporated. We shall enumerate our findings here;

1. We have shown in an analytic way that, in the confined phase with the vanishing Polyakov loop, the chiral symmetry should be spontaneously broken at any temperature in the Gocksch-Ogilvie model for both fundamental and adjoint quarks.

2. We discussed qualitatively how the quark contribution to the effective action can lower the deconfinement transition temperature.
3. In the case of fundamental quarks we have acquired the behavior of the order parameters as functions of the temperature and their slopes by differentiating with respect to the temperature. Then we found the peaks of the slope for the Polyakov loop and for the chiral order parameter located at the same pseudo-critical temperature.
4. Physical implication of the coincidence of the pseudo-critical temperatures has proved to be twofold: One is the deconfinement dominance where the remnant of the first order deconfinement transition would govern the behavior of the order parameters around T_c . The other is the chiral dominance where the second order chiral phase transition would be responsible for the realization of the simultaneous jump of the order parameters around T_c . We speculate that the real world corresponds to an intermediate admixture between the deconfinement dominance and the chiral dominance.
5. In the case of adjoint quarks we have found that the deconfinement transition is seen clearly of first order and that the chiral phase transition of second order occurs at higher temperature than the deconfinement transition does. It is apparent that the deconfinement temperature is substantially lowered from T_d to T_d^{**} , as expected, and the difference $T_d - T_d^{**}$ is insensitive to the current quark mass m_q as far as m_q is smaller than the scalar condensate (i.e. the constituent quark mass) or the temperature.

Some comments are in order. We will address our conjecture here that the finding 1 would be generalized so that we can prove the chiral symmetry breaking in the confined phase only using the property of the group integration, or, the Haar measure. Also it would be interesting to make sure whether 1 is realized in the lattice simulation. Such simulations will be feasible, in principle, if once we can examine the chiral symmetry breaking with a constraint imposed on the expectation value of the Polyakov loop, i.e., $\langle \text{Tr}_c L \rangle = 0$.

As for 3, we must improve the mean field approximation, especially the ansatz of the mean field action, to reproduce the coincidence of the pseudo-critical temperatures in the genuine susceptibility. This is a task for the future.

It would be fascinating from 4 to consider the possibility of the deconfinement dominance realizing in the lattice simulation because we can investigate the nature of the deconfinement around $T_c \simeq T_d^*$ and the nature of the chiral restoration around $T_\chi > T_c$ separately. In order to achieve such a situation, we have to make some modifications to the lattice QCD either to lower T_d^* or to raise T_χ . The problem of how to put the idea into practice is beyond the scope of the present paper.

Although it is rather academic, we finally remark about the possible relevance to physics on the critical end point (CEP). Recently the CEP, that is the terminal point of the first order transition, is paid much attention to in the realistic QCD phase diagram [28]. The location of the CEP is determined in part in the lattice QCD simulation at finite temperature and density [29]. The CEP can also emerge as the strange quark mass is varied in the three-flavor chiral phase transition [30].

Here we will draw attention to another chance to be confronted with the CEP, namely, the point where the deconfinement transition ceases to be first order with massive dynamical quarks. Our numerical analysis in the Gocksch-Ogilvie model predicts that the critical quark mass $m_q^c \sim 300$ MeV for Parameter I and $m_q^c \sim 700$ MeV for Parameter II. Actually there exist some lattice measurements to determine the critical mass of the CEP: In Ref. [31] $m_q^c \simeq 900$ MeV is concluded, while Ref. [32] reads $m_q^c \simeq 400$ MeV in more improved analyses with two-flavor quarks. The results in Ref. [32] is consistent with our estimate of m_q^c . In the one-flavor QCD simulation $m_q^c \simeq 1.4$ GeV is reported [33]. As for the three-flavor case [34], the situation becomes somewhat subtle because not only the deconfinement transition with heavy quarks but also the chiral phase transition with light quarks can be of first order. We anticipate that the property of the CEP in the deconfinement transition might be intriguing from the point of view of the glueball physics at finite temperature [35, 36].

In view of the prosperous descriptions as listed above, we can regard the Gocksch-Ogilvie model as a promising implement to afford a conceptual clue to the relation between the deconfinement transition and the chiral phase transition. It would be intriguing to make progress in applying the model to the system at finite density.

Acknowledgments

The author, who is supported by the Japan Society for the Promotion of Science for Young Scientists, would like to thank T. Hatsuda and S. Sasaki and Y. Nishida for discussions. He thanks T. Kunihiro for his sincere encouragement and warm hospitality at Yukawa Institute for Theoretical Physics.

APPENDIX A: CONSTRUCTION OF THE GOCKSCH-OGILVIE MODEL

In order to make this paper self-contained, we shall explain how to construct the Gocksch-Ogilvie model explicitly by following the derivation of Refs. [16, 21]. This would be useful to clarify what approximation is implicitly presumed. The model is formulated on the lattice. The strong coupling expansion is readily feasible on the lattice to lead to the quark confining property, i.e., the area law of the Wilson loop. Although the real world is actually in the weak coupling regime, numerical studies in the lattice QCD have revealed that even the strong coupling expansion should be likely to give a plausible picture relevant to the real world. The spontaneous breaking of the chiral symmetry can be described on the lattice as well by means of the double expansion of strong coupling and large dimensionality [16, 17]. Thus we can expect that an effective action suitable for discussing the relation between the Polyakov loop and the chiral order parameter will be available if once we bring together those assets on the lattice. This is the starting point to construct the Gocksch-Ogilvie model.

We adopt the staggered fermion in order to approach the chiral limit in a plain manner and also in order to take advantage of the simplicity in regard to the spin structure. The action on the lattice is given by the gluonic part;

$$S_G[U] = \frac{2N_c}{g^2} \sum_{n,(\mu,\nu)} \left\{ 1 - \frac{1}{N_c} \text{ReTr}_c U_{\mu\nu}(n) \right\}, \quad U_{\mu\nu}(n) = U_\nu^\dagger(n) U_\mu^\dagger(n + \hat{\nu}) U_\nu(n + \hat{\mu}) U_\mu(n) \quad (\text{A1})$$

for $N_c \geq 3$ and the staggered quark part;

$$\begin{aligned} S_F[U_d, U_i, \bar{\chi}, \chi] &= m_q \sum_n \bar{\chi}(n) \chi(n) + \frac{1}{2} \sum_{n, \mu > 0} \eta_\mu(n) \bar{\chi}(n) \{ U_\mu(n) \chi(n + \hat{\mu}) - U_\mu^\dagger(n - \hat{\mu}) \chi(n - \hat{\mu}) \} \\ &= m_q \sum_n \bar{\chi}(n) \chi(n) + \frac{1}{2} \sum_n \eta_d(n) \bar{\chi}(n) \{ U_d(n) \chi(n + \hat{d}) - U_d^\dagger(n - \hat{d}) \chi(n - \hat{d}) \} \\ &\quad - \sum_{n, i \neq d} \text{Tr}_c \left\{ \bar{\Phi}_i(n) U_i(n) + \Phi_i(n) U_i^\dagger(n) \right\}, \end{aligned} \quad (\text{A2})$$

where

$$\begin{aligned} \{ \Phi_i(n) \}_{ab} &= \frac{1}{2} \eta_i(n + \hat{i}) \bar{\chi}_b(n + \hat{i}) \chi_a(n), \\ \{ \bar{\Phi}_i(n) \}_{ab} &= -\frac{1}{2} \eta_i(n) \bar{\chi}_b(n) \chi_a(n + \hat{i}). \end{aligned} \quad (\text{A3})$$

We have divided the quark action into one part with U_i and the other part without U_i for later convenience. a, b run in the color space. We can handle the quark action in the adjoint representation by replacing the link variables in the covariant derivatives by

$$U_{ab}^{(\text{adj.})} = 2 \text{tr} \left[t_a U t_b U^\dagger \right]. \quad (\text{A4})$$

Roughly speaking, the adjoint quark is like a color octet fermionic meson composed of a quark and an anti-quark in the fundamental representation ($\mathbf{8}$ out of $\mathbf{3} \otimes \bar{\mathbf{3}} = \mathbf{1} \oplus \mathbf{8}$). We will write the link variable as $U^{(r)}$ in the r representation.

In order to attain the effective action in terms of the Polyakov loop and the quark field, we must integrate over the spatial link variable U_i . Then the effective partition function is written as

$$\begin{aligned} Z_{\text{eff}}^{(r)}[U_d, \chi, \bar{\chi}] &= \int \mathcal{D}U_i e^{-S_G[U_d, U_i] - S_F[U, \chi, \bar{\chi}]} \\ &= \exp \left[m_q \sum_n \bar{\chi}(n) \chi(n) + \frac{1}{2} \sum_n \eta_d(n) \bar{\chi}(n) \{ U_d^{(r)}(n) \chi(n + \hat{d}) - U_d^{(r)\dagger}(n - \hat{d}) \chi(n - \hat{d}) \} \right] \\ &\quad \times \int \mathcal{D}U_i \exp \left[-S_G[U_d, U_i] + \sum_{n, i \neq d} \text{Tr}_c \left\{ \bar{\Phi}_i(n) U_i^{(r)}(n) + \Phi_i(n) U_i^{(r)\dagger}(n) \right\} \right]. \end{aligned} \quad (\text{A5})$$

In the strong coupling expansion, the spatial plaquette can be neglected, which can be perceived more on the asymmetric lattice [37]. An extreme case of such asymmetric lattice methods is the Hamiltonian formalism where only the temporal plaquette remains in the strong coupling limit. Then the U_i integration part can be expanded as

$$\int \mathcal{D}U_i \sum_{p,q} \frac{1}{p!q!} \left[\frac{1}{g^2} \sum_{n, i \neq d} \text{Tr}_c \left\{ U_{id}(n) + U_{id}^\dagger(n) \right\} \right]^p \left[\sum_{n, i \neq d} \text{Tr}_c \left\{ \bar{\Phi}_i U_i^{(r)}(n) + \Phi_i(n) U_i^{(r)\dagger}(n) \right\} \right]^q. \quad (\text{A6})$$

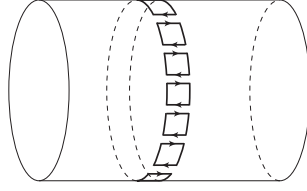


FIG. 7: Graphical representation of the configuration contributing to the effective action in the lowest order of the strong coupling. The torus stands for the thermal (temporal) S^1 and the spatial R^3 .

The Taylor expansion of the gluonic part (series in p) obviously corresponds to the strong coupling ($1/g^2$) expansion. As we explain soon below, the Taylor expansion of the quark part (series in q) corresponds to the large dimensional ($1/d$) expansion. We specify the order of the double expansion as follows; first, we perform the large dimensional expansion. Then, in each expanded term we take the leading contribution of the strong coupling expansion.

For the zeroth order ($q = 0$) term of the $1/d$ expansion, the leading contribution left after the U_i integration derives from the configuration with the plaquettes wrapping around the thermal (temporal) torus ($p = N_\tau$), as depicted in Fig. 7. As a result, the U_i integration for the $q = 0$ term is [12]

$$1 + \left(\frac{1}{g^2 N_c} \right)^{N_c} \sum_{\text{n.n.}} \text{Tr}_c L(\vec{n}) \text{Tr}_c L^\dagger(\vec{m}). \quad (\text{A7})$$

The next contribution comes from the second order ($q = 2$) term. Since two link variables in the covariant derivative can form a color singlet pair, the leading contribution in the strong coupling expansion is simply the zeroth ($p = 0$) term. As a result, we have

$$\begin{aligned} & \int \mathcal{D}U_i \left[\sum_{n,i \neq d} \text{Tr}_c \left\{ \bar{\Phi}_i U_i^{(r)}(n) + \Phi_i(n) U_i^{(r)\dagger}(n) \right\} \right]^2 \\ &= \sum_{n,i \neq d} \frac{1}{\text{dim}(r)} \text{Tr}_c \{ \bar{\Phi}_i(n) \Phi_i(n) \} = \sum_{n,i \neq d} \frac{\text{dim}(r)}{2(d-1)} M(n) M(n + \hat{i}), \end{aligned} \quad (\text{A8})$$

where the mesonic composite field is defined by

$$M(n) = \frac{1}{\text{dim}(r)} \sqrt{\frac{d-1}{2}} \sum_{a=1}^{\text{dim}(r)} \chi_a(n) \bar{\chi}_a(n). \quad (\text{A9})$$

In Eq. (A8) the dimension number of the r representation is denoted by $\text{dim}(r)$ as in the text. It should be noted that, for adjoint quarks, only such a mesonic interaction as $\text{Tr}_c \{ \bar{\Phi}_i \Phi_i \}$ survives not only because of the group integration with respect to U_i but also because of the properties of the Grassmann variables χ and $\bar{\chi}$.

At this stage it is easy to understand why such an expansion in q provides the large dimensional expansion. Since the meson should propagate with finite amplitude in the large dimensional limit, we must properly normalize $M(n)$ so as to have the factor $1/(d-1)$ in front of the term $M(n)M(n + \hat{i})$ (i runs from 1 to $d-1$). As a result, each time Φ_i , or M , appears in a term, the order of the term in the $1/d$ expansion should be lowered. Thus the Taylor expansion of the exponential of the quark action amounts to the expansion in $1/d$.

We combine Eqs. (A5)–(A8) and exponentiate the expanded terms. Then, using the identity,

$$\exp \left[\text{dim}(r) \sum_{m,n} \frac{1}{2} M(n) V(n, m) M(m) \right] = \int \mathcal{D}\lambda \exp \left[-\text{dim}(r) \sum_{m,n} \left\{ \frac{1}{2} \lambda(n) V(n, m) \lambda(m) - \lambda(n) V(n, m) M(m) \right\} \right], \quad (\text{A10})$$

we can reach the effective partition function;

$$\begin{aligned}
Z_{\text{eff}}^{(r)}[U_d, \lambda] = & \int \mathcal{D}\chi \mathcal{D}\bar{\chi} \exp \left[-S_{\text{eff}}^{(G)}[L] - \frac{\dim(r)}{2} \sum_{m,n} \lambda(n) V(n, m) \lambda(m) \right. \\
& - \frac{1}{2} \sum_n \eta_d(n) \left\{ \bar{\chi}(n) U_d^{(r)}(n) \chi(n + \hat{d}) - \bar{\chi}(n + \hat{d}) U_d^{(r)\dagger}(n) \chi(n) \right\} \\
& \left. - \sum_n \bar{\chi}(n_d) \left\{ \sqrt{\frac{d-1}{2}} \sum_m \lambda(m) V(m, n) + m_q \right\} \chi(n_d) \right]. \tag{A11}
\end{aligned}$$

From Eq. (A7), the effective action in terms of the Polyakov loop, $S_{\text{eff}}^{(G)}[L]$, is given by

$$S_{\text{eff}}^{(G)}[L] = -J \sum_{\text{n.n.}} \text{Tr}_c L(\vec{n}) \text{Tr}_c L^\dagger(\vec{m}). \tag{A12}$$

where J is given by

$$J = \left(\frac{1}{g^2 N_c} \right)^{N_\tau} = e^{-\sigma a/T}. \tag{A13}$$

Here we have used the familiar expression for the string tension in the strong coupling expansion, i.e., $\sigma a^2 = \ln[g^2 N_c]$. We will fix the lattice spacing a as a cut-off parameter and vary the temperature by changing the number of lattice sites in the thermal direction, N_τ .

In Eq. (A11) the hopping propagator of the meson fields $V(n, m)$ is defined in Eq. (4). Since the quark part takes a bilinear form in Eq. (A11), we can perform the integration with respect to the quark fields explicitly under the approximation that λ is *independent* of n_d (time). This approximation is indeed reasonable as long as we employ the mean field approximation and treat λ as a constant, in the same sense as the sigma meson field in the relativistic nuclear many-body system. We would emphasize, however, that this approximation might be invalid when the meson fluctuation is concerned. In other words, we should not use the action of the Goksch-Ogilvie model to estimate the meson fluctuation (loop) effect.

Then after the integration we can reach the Goksch-Ogilvie model given in Eq. (1) by using $S_{\text{eff}}^{(r)} = -\ln Z_{\text{eff}}^{(r)}$. We should remark that N_f in the effective action (1) is the number of flavors introduced from the phenomenological point of view. We cannot avoid having four degenerate flavors per a single component of the staggered fermion. The logarithmic contribution in Eq. (1) results from the quark integration in Eq. (A11). The coefficient $N_f/4$ in front of the logarithmic term effectively adjusts the number of flavors in the integration with respect to the quark fields χ .

It is worth mentioning that σ in Eq. (A13) is constant and fixed at the empirical value at zero temperature. The string tension of the linear potential defined by the Polyakov loop correlation function, nevertheless, depends on the temperature and decreases with the temperature increasing. In reality the string tension should have temperature dependence in addition due to the vibrations of the flux tube. The higher temperature the system is heated up at, the more furious the vibration becomes. Such effects of the string vibration are to be described by the higher order contributions in the strong coupling expansion. If we take account of the spatial link variables, or the magnetic plaquettes in the Hamiltonian formalism, to exceed the leading order contribution of Eq. (A7), we can incorporate temperature dependence coming from the string vibration in principle. Since the essence on the deconfinement transition is already concentrated in the effective action (A7), we simply neglect any spatial fluctuation in the present model.

If we proceeded to the higher order contribution of the strong coupling expansion, we would have the fat meson contributions as shown in Fig. 8. Neglecting such fat excitations implies that we neglect the structural change of mesons in the temporal direction. In other words, the meson hopping in the spatial direction have no extent in the temporal direction and is always color-confined.

APPENDIX B: CHIRAL CONDENSATE

The chiral condensate can be calculated as

$$\Psi = \langle \bar{\chi} \chi \rangle = -\frac{1}{\dim(r) N^d} \frac{d}{dm_q} \ln Z_{\text{eff}}^{(r)} \sim \frac{1}{\dim(r)} \frac{df_{\text{mf}}^{(r)}(x, \bar{\lambda}_0)}{dm_q}, \tag{B1}$$

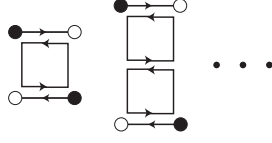


FIG. 8: Examples of neglected excitations as a result of the approximation. The vertical and horizontal lines represent the temporal (thermal) and spatial link variables respectively.

where $\bar{\lambda}_0$ is the solution of the stationary condition (see Eq. (9)),

$$\left. \frac{\partial f_{\text{mf}}^{(r)}(x, \bar{\lambda})}{\partial \bar{\lambda}} \right|_{\bar{\lambda}=\bar{\lambda}_0} = \text{dim}(r) + \sqrt{\frac{d-1}{2}} \cdot \left. \frac{\partial f_{\text{mf}}^{(r)}(x, \bar{\lambda})}{\partial m_q} \right|_{\bar{\lambda}=\bar{\lambda}_0} = 0. \quad (\text{B2})$$

Then, using the stationary condition, we can readily obtain

$$\begin{aligned} \Psi &= \frac{1}{\text{dim}(r)} \frac{d f_{\text{mf}}^{(r)}(x, \bar{\lambda}_0)}{d m_q} = \frac{1}{\text{dim}(r)} \frac{\partial f_{\text{mf}}^{(r)}(x, \bar{\lambda}_0)}{\partial m_q} \\ &= \frac{1}{\text{dim}(r)} \sqrt{\frac{2}{d-1}} \left(\frac{\partial f_{\text{mf}}^{(r)}(x, \bar{\lambda}_0)}{\partial \bar{\lambda}_0} - \text{dim}(r) \bar{\lambda}_0 \right) = -\sqrt{\frac{2}{d-1}} \bar{\lambda}_0. \end{aligned} \quad (\text{B3})$$

Actually this result does not depend on the concrete form of the free energy. We can immediately reach the same result from Eq. (A10) by infinitesimally shifting the integration variable. Thus, the scalar condensate is simply proportional to the chiral condensate.

In the same way, we can relate our susceptibility χ_λ defined in Eq. (26) to the conventional chiral susceptibility χ_Ψ which is given by

$$\begin{aligned} \chi_\Psi &= \frac{1}{[\text{dim}(r)]^2} \frac{d^2 f_{\text{mf}}^{(r)}(x, \bar{\lambda}_0)}{d m_q^2} \\ &= \frac{1}{[\text{dim}(r)]^2} \left\{ \left(\frac{d \bar{\lambda}_0}{d m_q} \right)^2 \frac{\partial^2 f_{\text{mf}}^{(r)}(x, \bar{\lambda}_0)}{\partial \bar{\lambda}^2} + \frac{\partial^2 f_{\text{mf}}^{(r)}(x, \bar{\lambda}_0)}{\partial m_q^2} \right\}. \end{aligned} \quad (\text{B4})$$

Differentiating the first equation of Eq. (B2) by $\bar{\lambda}$ and m_q respectively and combining them, we can reach the relation;

$$\frac{d \bar{\lambda}_0}{d m_q} = \text{dim}(r) \sqrt{\frac{2}{d-1}} \left(\frac{\partial^2 f_{\text{mf}}^{(r)}(x, \bar{\lambda}_0)}{\partial \bar{\lambda}^2} \right)^{-1} - \sqrt{\frac{2}{d-1}}. \quad (\text{B5})$$

In the vicinity of the critical temperature with small current quark mass ($m_q \sim 0$), the curvature of the free energy (second partial derivative of the free energy) with respect to the scalar meson field approaches zero. Consequently the first term in the brackets in Eq. (B4) dominates to result in

$$\chi_\Psi \sim \frac{2}{d-1} \left(\frac{\partial^2 f_{\text{mf}}^{(r)}(x, \bar{\lambda}_0)}{\partial \bar{\lambda}^2} \right)^{-1} = \frac{2\beta}{d-1} (\langle \lambda^2 \rangle - \langle \lambda \rangle^2). \quad (\text{B6})$$

APPENDIX C: ZERO TEMPERATURE EXPRESSIONS FOR N_f FLAVORS

Here we briefly summarize the zero temperature expressions given in Ref. [16] with modifications for N_f flavors. The effective potential in terms of the chiral order parameter $\bar{\lambda}$ is modified at zero temperature into

$$V_{\text{eff}}(\bar{\lambda}) = \frac{N_c}{2} \bar{\lambda}^2 - \frac{N_c N_f}{4} \ln \left[\bar{\lambda} + \sqrt{\frac{2}{d}} m_q \right], \quad (\text{C1})$$

from which the stationary value of $\bar{\lambda}$ is obtained as

$$\bar{\lambda} = -\frac{m_q}{\sqrt{2d}} + \sqrt{\frac{N_f}{4} + \frac{m_q^2}{2d}}. \quad (\text{C2})$$

If we rescale $m_q = \tilde{m}_q \sqrt{N_f/4}$, then the N_f dependence in $\bar{\lambda}$ can be factorized as

$$\bar{\lambda} = \sqrt{\frac{N_f}{4}} \left(-\frac{\tilde{m}_q}{\sqrt{2d}} + \sqrt{1 + \frac{\tilde{m}_q^2}{2d}} \right), \quad (\text{C3})$$

where the expression in the brackets is nothing but that of Ref. [16] without any care about the flavor number. Thus we can expect that most of modifications could be absorbed in the rescale of the current quark mass $m_q \rightarrow \tilde{m}_q$. In fact, the hadron spectrum for N_f flavors is given by

$$\begin{aligned} \cosh M_p &= d \left\{ \frac{4}{N_f} \left(\frac{m_q}{\sqrt{2d}} + \sqrt{\frac{N_f}{4} + \frac{m_q^2}{2d}} \right)^2 - 1 \right\} + 2p + 1 \\ &= d \left\{ \left(\frac{\tilde{m}_q}{\sqrt{2d}} + \sqrt{1 + \frac{\tilde{m}_q^2}{2d}} \right)^2 - 1 \right\} + 2p + 1. \end{aligned} \quad (\text{C4})$$

Therefore the hadron spectrum necessary for fixing the model parameters is not affected by the number of flavors.

APPENDIX D: EXPANSIONS

We shall discuss the expansion in terms of $1/\alpha$ for the integrations $\tilde{I}_n(x; \alpha)$ and $\tilde{I}_n^m(x; \alpha)$ given by Eqs. (10) and (11). Such expansions are exploited for the numerical calculation with adjoint quarks. It is somewhat inefficient to attack the integration given in Eq. (11) directly and thus we expand the free energy in terms of $1/\alpha$. We can obtain such an expansion from Eqs. (10) and (11) up to third order as

$$\begin{aligned} \tilde{I}_n(x; \alpha) &= \frac{1}{2\alpha} \{I_{n+1}(x) + I_{n-1}(x)\} - \frac{1}{8\alpha^2} \{I_{n+2}(x) + 2I_n(x) + I_{n-2}(x)\} \\ &\quad + \frac{1}{24\alpha^3} \{I_{n+3}(x) + 3I_{n+1}(x) + 3I_{n-1}(x) + I_{n-3}(x)\}, \end{aligned} \quad (\text{D1})$$

$$\begin{aligned} \tilde{I}_n^m(x; \alpha) &= \frac{1}{2\alpha} \{I_{m+1}(x)I_{n-1}(x) + I_{m-1}(x)I_{n+1}(x)\} \\ &\quad - \frac{1}{8\alpha^2} \{I_{m+2}(x)I_{n-2}(x) + 2I_m(x)I_n(x) + I_{m-2}(x)I_{n+2}(x)\} \\ &\quad + \frac{1}{24\alpha^3} \{I_{m+3}(x)I_{n-3}(x) + 3I_{m+1}(x)I_{n-1}(x) \\ &\quad + 3I_{m-1}(x)I_{n+1}(x) + I_{m-3}(x)I_{n+3}(x)\}. \end{aligned} \quad (\text{D2})$$

We can test the reliability of such approximations by comparing with the full (not expanded) numerical results. In Fig. 9 we show the full numerical result obtained from the free energy (9) directly (dashed curve) and the approximate one with the expanded free energy (solid curve) in the case of fundamental quarks with Parameter I. It is obvious from the figure that the expansion (D1) works well except for the behavior of the chiral order parameter around the chiral phase transition. Thus we can presume that the expansion (D2) will work enough for adjoint quarks as well, at least, to see the qualitative features.

-
- [1] There are lots of reviews and textbooks on QGP physics. See for example; J.W. Harris and B. Müller, *Ann. Rev. Nucl. Part. Sci.* **46**, 71 (1996).
C.Y. Wong, *Introduction to High-Energy Heavy-Ion Collisions*, (World Scientific, Singapore, 1994).
- [2] A. Casher, *Phys. Lett. B* **83**, 395 (1979).
G. 't Hooft, in: *Recent Developments in Gauge Theories*, Eds. G. 't Hooft et al., (Plenum, New York, 1980).
- [3] A.M. Polyakov, *Phys. Lett. B* **72**, 477 (1978).
L. Susskind, *Phys. Rev. D* **20**, 2610 (1979).
B. Svetitsky and L.G. Yaffe, *Nucl. Phys.* **B210** [FS6], 423 (1982).
B. Svetitsky, *Phys. Rep.* **132**, 1 (1986).
- [4] L.D. McLerran and B. Svetitsky, *Phys. Lett. B* **98**, 195 (1981); *Phys. Rev. D* **24**, 450 (1981).
J. Kuti, J. Polonyi, and K. Szlachányi, *Phys. Lett. B* **98**, 199 (1981).

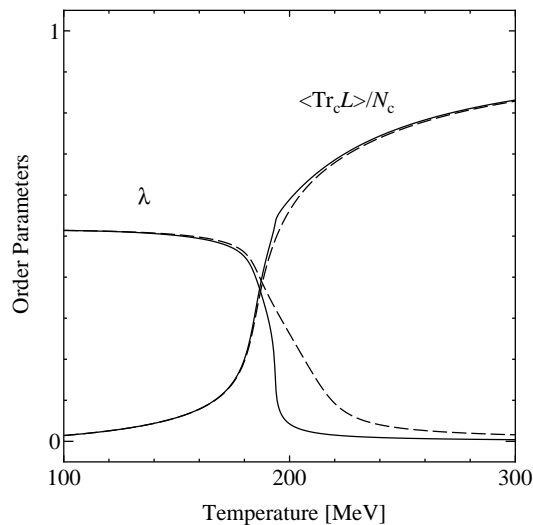


FIG. 9: Comparison between the numerical results of Ref. [22] (shown by dashed curves) and the approximate estimates by the free energy expanded in terms of $1/\cosh(N_\tau E)$ up to third order (shown by solid curves).

- [5] A.V. Smilga, *Ann. Phys.* **234**, 1 (1994).
- [6] O. Kaczmarek, F. Karsch, P. Petreczky, and F. Zantow, *Phys. Lett. B* **543**, 41 (2002).
- [7] N. Weiss, *Phys. Rev. D* **24**, 475 (1981); *Phys. Rev. D* **25**, 2667 (1982).
V.M. Belyaev, *Phys. Lett. B* **254**, 153 (1991).
T. Bhattacharya, A. Gocksch, C.P. Korthals Altes, and R.D. Pisarski, *Nucl. Phys.* **B383**, 497 (1992).
C.P. Korthals Altes, *Nucl. Phys.* **B420**, 637 (1994).
- [8] K. Fukushima and K. Ohta, *J. Phys. G* **26**, 1397 (2000).
- [9] A. Gocksch and R.D. Pisarski, *Nucl. Phys.* **B402**, 657 (1993).
- [10] H. Reinhardt, *Mod. Phys. Lett. A* **11**, 2451 (1996).
- [11] F. Lenz and M. Thies, *Ann. Phys.* **268**, 308 (1998).
- [12] J. Polonyi and K. Szlachanyi, *Phys. Lett. B* **110**, 395 (1982).
- [13] M. Gross, *Phys. Lett. B* **132**, 125 (1983); M. Gross, J. Bartholomew, and D. Hochberg, "SU(N) deconfinement transition and the N state clock model," preprint EFI-83-35-CHICAGO (1983).
- [14] T. Banks and A. Ukawa, *Nucl. Phys.* **B225** [FS9], 145 (1983).
- [15] See for example;
S.P. Klevansky, *Rev. Mod. Phys.* **64**, 649 (1992).
T. Hatsuda and T. Kunihiro, *Phys. Rep.* **247**, 221 (1994).
H. Meyer-Ortmanns, *Rev. Mod. Phys.* **68**, 473 (1996).
- [16] H. Kluberg-Stern, A. Morel, and B. Petersson, *Nucl. Phys.* **B215** [FS7], 527 (1983).
- [17] P.H. Damgaard, N. Kawamoto, and K. Shigemoto, *Nucl. Phys.* **B264**, 1 (1986).
N. Bilić, F. Karsch, and K. Redlich, *Phys. Rev. D* **45**, 3228 (1992).
- [18] F. Karsch and E. Laermann, *Phys. Rev. D* **50**, 6954 (1994).
S. Aoki, M. Fukugita, S. Hashimoto, N. Ishizuka, Y. Iwasaki, K. Kanaya, Y. Kuramashi, H. Mino, M. Okawa, A. Ukawa, and T. Yoshié, *Phys. Rev. D* **57**, 3910 (1998).
- [19] H. Satz, *Nucl. Phys.* **A642**, 130 (1998).
- [20] S. Digal, E. Laermann, and H. Satz, *Eur. Phys. J. C* **18**, 583 (2001).
- [21] A. Gocksch and M. Ogilvie, *Phys. Rev. D* **31**, 877 (1985).
- [22] K. Fukushima, *Phys. Lett. B* **553**, 38 (2003).
- [23] K. Fukushima, *Ann. Phys.* **304**, 72 (2003).
- [24] J. Kogut, J. Polonyi, H.W. Wyld, and D.K. Sinclair, *Phys. Rev. Lett.* **54**, 1980 (1985).
F. Karsch and M. Lütgemeier, *Nucl. Phys.* **B550**, 449 (1999).
- [25] F. Green and F. Karsch, *Nucl. Phys.* **B238**, 297 (1984).
- [26] M. Creutz, *Quarks, gluons and lattices*, (Cambridge University Press, England, 1983), Chap. 14.
- [27] J. Kogut, M. Snow, and M. Stone, *Nucl. Phys.* **B200**, 211 (1982).
- [28] M. Stephanov, K. Rajagopal, and E. Shuryak, *Phys. Rev. Lett.* **81**, 4816 (1998); *Phys. Rev. D* **60**, 114028 (1999).
B. Berdnikov and K. Rajagopal, *Phys. Rev. D* **61**, 105017 (2000).
K. Fukushima, *Phys. Rev. C* **67**, 025203 (2003).
Y. Hatta and T. Ikeda, *Phys. Rev. D* **67**, 014028 (2003).
Y. Hatta and M.A. Stephanov, e-print: [hep-ph/0302002](https://arxiv.org/abs/hep-ph/0302002).

- [29] Z. Fodor and S.D. Katz, *J. High Energy Phys.* **03**, 014 (2002).
- [30] S. Gavin, A. Gocksch, and R.D. Pisarski, *Phys. Rev. D* **49**, R3079 (1994).
- [31] P. Hasenfratz and F. Karsch, and I.O. Stamatescu, *Phys. Lett. B* **133**, 221 (1983).
- [32] N. Attig, B. Petersson, M. Wolff, and R.V. Gavai, *Z. Phys. C* **40**, 471 (1988).
- [33] C. Alexandrou, A. Boriçi, A. Feo, P. de Forcrand, A. Galli, F. Jegerlehner, and T. Takaishi, *Phys. Rev. D* **60**, 034504 (1999).
- [34] F. Karsch, E. Laermann, and C. Schmidt, *Phys. Lett. B* **520**, 41 (2001).
- [34] F. Karsch, C. Schmidt, and S. Stickan, *Comput. Phys. Commun.* **147**, 451 (2002).
- [35] S. Datta and S. Gupta, *Nucl. Phys.* **B534**, 392 (1998).
- [35] N. Ishii, H. Suganuma, and H. Matsufuru, *Phys. Rev. D* **66**, 014507 (2002); *Phys. Rev. D* **66**, 094506 (2002).
- [36] Y. Hatta, in private communications.
- [37] M. Billó, M. Casell, A. D’Adda, and S. Panzeri, *Nucl. Phys.* **B472**, 163 (1996).
- [38] We would like to comment upon the subtleties encountered in defining and interpreting the Polyakov loop in a continuum theory. Unless the color group is $SU(2)$, $\langle \text{Tr}_c L \rangle$ may be complex, while $\exp[-\beta f_q]$ is always real. Moreover it is known that $\langle \text{Tr}_c L \rangle$ without any proper renormalization goes to zero in the continuum limit. As emphasized in Ref. [5] what is meaningful is the correlation function of the Polyakov loops, from which the inter-quark potential can be inferred. Although the Polyakov loop might make little sense as it is, however, the properly renormalized Polyakov loop can be defined by the correlation function of the Polyakov loops with infinite separation. Recently it has been actually demonstrated that the renormalized Polyakov loop is well-behaved as an order parameter [6]. We will not go into this issue in the present paper since we take an ansatz for the mean field approximation (the Polyakov loop is then chosen as real) and have an explicit cut-off parameter of the lattice spacing here.
- [39] The author thanks T. Kunihiro for the derivation of these integration formulae.
- [40] The expansion given by Eq. (16) of Ref. [22] should be corrected; N_c replaced by $N_c - 2$ and a factor $1/\sqrt{2}$ inserted. Thus the linear term disappears in the case of $N_c = 2$.